Int. J. Econ. Environ. Geol. Vol. 10 (1) 84-92, 2019

Journal home page: www.econ-environ-geol.org

Open Access

ISSN: 2223-957X

Determination of Underground Structure and Migration of Hot Plumes Contaminating Fresh Water Using Vertical Electrical Survey (VES) and Magnetic Survey, A Case Study of Tattapani Thermal Spring, Azad Kashmir

Mehboob ur Rashid[1]*, Waqas Ahmad[2], Muhammad Jawad Zeb[1], Naghmah Haider[1], Asad Khan[3], Sajjad Khan[1]

[1]Geoscience Advance Research Laboratories Islamabad, Geological Survey of Pakistan
[2]National Centre of Excellence in Geology, University of Peshawar, Pakistan
[3]Department of Geology, FATA University, Dara Adam Khel, Pakistan

*Email: mehboobgeo89@gmail.com

Received: *19 December, 2018* ***Accepted:*** *21 March, 2019*

Abstract: A geophysical survey was carried out at Tattapani thermal spring Azad Kashmir to delineate structure, thickness, depth, lithology and migration of hot plumes contaminating fresh water. The study area was investigated by Vertical Electrical Sounding (VES) using schlumberger array at 21 locations arranged in ten profiles to a maximum depth of 500 m and 200 magnetic observations. The extension and tectonic setup of thermal spring was mapped by geoelectrical litho sections, subsurface geological sections (20m, 20-100m and 100-500m) pseudo section, apparent resistivity map, geoelectrical parameters, statistical distribution of apparent resistivity, total magnetic intensity and anomaly map. The data show that Tattapani hot spring is concentrated along the fault line delineated by geoelectrical litho sections and magnetic section with value of -120 nT to -300 nT, total field intensity of 50000-50450 nT and confirm by macro anisotropy (1.0 to 2.7). The geoelectrical lithological section portrays that study area comprises lithological fabric of dolomite (≥400 ohm.m), sandstone (150-200 ohm.m), clay (80-150 ohm.m), Shaley clay (50-80) and shale (≤ 50). The Thermal Plumes (10-70 ohm.m) were pictured by resistivity section and pseudo section at average depth of 30-60 m and showing migration of hot plumes in the North-Eastern direction contaminating fresh water (100-200 ohm.m). The longitudinal conductance (0.95-15 mhos), transverse resistance (20-300 ohm.m^2) are seen having maximum value in the North-Eastern and North-Western side of the study area. The study also shows that fresh ground water is mostly concentrated in sandstone (150-200 ohm.m), dolomite (≥400 ohm.m) and lies above the thermal plumes and thus highly prone to contamination due to upwelling of thermal water.

Keywords: Thermal spring, hot plumes, vertical electrical sounding, magnetic survey, Azad Kashmir.

Introduction

Groundwater is a vital resource occurring naturally, entrapped by underground lithology, channelized by porosity, permeability and fracture to the surface (Oseji et al., 2006). It is important for sustaining life by providing drinking water to living communities, establishing irrigation system and balancing of ecosystem. The world water system is encountering ominous threat and will startle the global community in guise of imminent water paucity. According to World Resource Institute, about a billion people inhabit water scarce domains and by 2025 this total will flower to the zenith of 3.5 billion enduring water deficiency. The potable groundwater is deteriorated by the ceaseless inundation of pollutants, primarily ramification of urbanization, industrialization, agriculture and anthropogenic activities. The quality of groundwater is contingent on its chemical composition and solvated minerals group (Akaninyene and Igboekwe, 2012). These naturally dissolved ingredients are vital for human organization, with increase above threshold making it unhealthy for drinking.

With the advent of modern technology aided by advanced instrumentation associated with numerical modelling, the subsurface hydrogeological condition is widely investigated by applying integrated approach of geophysical techniques using Vertical Electrical Sounding (VES) and Magnetic Survey (Araffa et al., 2012; Maury and Balaji, 2014). The VES works on the principle of resistivity contrast, controlled by geo-lithological properties (porosity, permeability, anisotropy, orientation of grains) showing strong correlation with resistivity distribution (Sikandar et al., 2010; Stollar and Roux, 1975; VenkataRao et al., 2014). The resistivity distribution has widely been used for mapping underground structures, groundwater contamination, lithology and environmental issues (Bradbury and Taylor, 1984; Koukadaki et al., 2007; Kundu et al., 2002; Sultan and Santos, 2008; Wilson et al., 2006). The magnetic survey is widely used to demarcate the concealed faults, lithological contacts, intrusion, ground water distribution and anomalous zones based on magnetic field of different materials (El All et al., 2015; He et al., 2014; Hewaidy et al., 2015).

In the current study an attempt has been made to unravel the underground structure and delineate the contaminated zones of ground water using integrated geophysical survey. The study is focused to address the subsurface lithological condition, groundwater resource (Fresh water / Hot water) and distribution of

hot water and its extension based on resistivity signature.

Study Area

The study area is part of district Kotli, Azad Kashmir and part of the Himalayan fold-thrust belt that lies between longitudes 73° 56′ 58″ to 73° 57′ 12″ E and latitudes 33° 36′ 27″ to 33° 37′ 02″ N of the Survey of Pakistan Toposheet No. 43-G/14. The topography of the study is uneven, characterized by rugged topography and undulating landscape with the height of 1400 m from mean sea level. The climate of the area is subtropical and humid having mean annual rainfall of 1400 mm, with maximum in monsoon season (Nadeem, 2015). The groundwater resource potential of the study area are natural springs and dug wells, which are recharged by river Poonch originating from the western foothills of Pir Panjal range.

The lithological units exposed in study area are mostly clastic sedimentary rocks of Cambrian to Tertiary age (Shah et al., 2007; Thakur et al., 2010) (Fig. 1). The oldest formation exposed is Abbottabad Formation of Cambrian age, mostly composed of cherty dolomite and quartzite. The Abbottabad Formation is unconformably overlain by Patala Formation of Paleocene age with lithological fabric of clay, shale and sandstone (Shah, 2009). The Tattapani thermal spring is concentrated on the north-western tip of Tattapani anticline, at the contact point between Patala and Abbottabad formations (Anees et al., 2015; Mughal et al., 2004). The Tattapani thermal spring oozes consistently for the last decades and is well known by its medicinal power due to the enrichment by sulphur and other dissolved minerals (Ahmad et al., 2002; Bakht, 2000; Hussain et al., 1994; Todaka et al., 1988). According to Public Health Engineering (PHE) department of Kotli, the quality of water is not good in the study area with chlorination done on regular basis of wells near river Poonch (Shah et al., 2004). The current study demarcates the zones of contamination by hot springs in surrounding area, which will aid in ground resource management and planning.

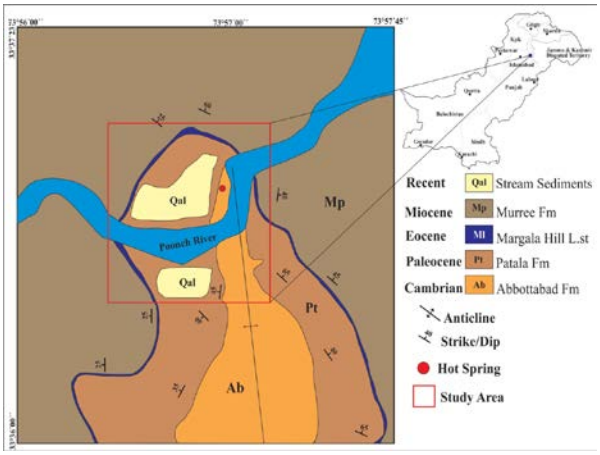

Fig. 1 Geological map covering part of Toposheet No. 43 G/14, showing the study area (Shah et al., 2007).

There is acute shortage of drinkable water and overall water risk is 4-5 by WRI report (Gassert et al., 2013). The thermal plumes with high dissolved content in the hot spring water (Anees et al., 2015) are migrating and contaminating the underground fresh reservoir, which is the only source of drinkable water of the study area.

Materials and Methods

Resistivity Survey

A detailed resistivity has been applied to have maximum coverage of the area, by adopting the techniques of Vertical Electrical Sounding (VES) using schlumberger electrode configuration (SEC). The SEC are very popular for delineating subsurface horizon, fracture zones, faults and ground resource management (Wilson et al., 2006), attributed due to its high depth of penetration and better resolution (Atakpo and Ayolabi, 2009; Ojelabi et al., 2002). The resistivity of rock is functional to its mineralogical fabric, fluid content, saturation, porosity and permeability (Arshad et al., 2007). The resistivity method uses direct current on the surface to image subsurface horizon based on resistivity contrast associated with zones of interest (Joshua et al., 2011). The instruments used in this study are TSQ-3 transmitter and RDC-10 receiver of Scintrex Canada, aided by generator, current steel electrodes and potential porous pots. The transmitters and receivers are operated in time domain mode with time interval of 2 seconds. In the study area a total of 21 VES are executed stacked along 10 profiles, to a maximum depth of 500 m depending upon the availability of space (Fig. 2). The current electrode spacing (AB) ranges from 6 to 500 m and potential electrode (MN) reaching 1.5 to 25 m.

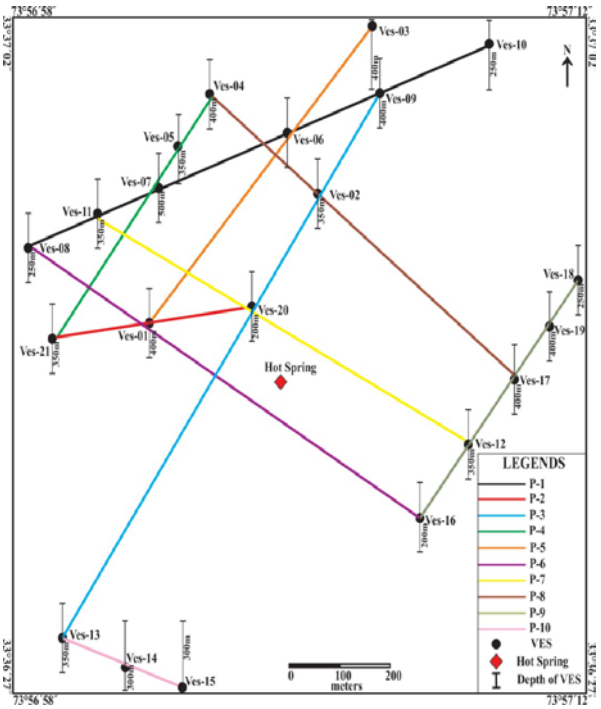

Fig. 2 Base map of the study area showing VES arranged along ten profiles (P-1 to P-10).

Magnetic Survey

A high resolution detailed magnetic survey is performed at grid interval of 100 or 50 meters to map Tattapani thermal spring in order to have overall subsurface structure and magnetic features of rock. The magnetic survey is widely used for the delineation of underground faults and tectonic structure based on the magnetic signatures (El All et al., 2015). The proton precession magnetometer G-856 of Geometric Canada was used for data acquisition on a regular North-South grid pattern of 50×50 m, with total observation points of 200. The data acquired during the field are processed and converted into meaningful form by applying all necessary correction for diurnal variation and latitude. The magnetic survey is performed to determine the tectonic control of thermal spring and correlating with resistivity data.

Results and Discussion

The VES data acquired during field survey is fed into modelling software using IPI2win by applying normal inversion iteration techniques to have final true resistivity curve with layer thickness and depth (Bobachev, 2002). The data are shown in the shape of sounding curve on a semi logarithmic graph with true resistivity on y-axis and electrode separation on x-axis. The geoelectrical lithosections of each VES are prepared as to portray the lithological variation along depth. The resistivity pseudo section and statistical distribution of apparent resistivity are also prepared to demarcate the lithological variation, migration of hot plumes and water resource delineation. The spatial distribution of apparent resistivity at 10 m, 20 m, 60 m, 80 m, 100 m and 200 m are generated to portray the trend of changing resistivity in the study area. Dar-zarrouk geoelectrical parameters are also determined and modelled using surfer software, to define the anisotropy and permeable beds help in movement of hot plumes and water conduction. The total magnetic intensity and total magnetic anomaly maps are also created, in order to interpret the structural control of lithology and concentration of thermal spring.

Geoelectrical Lithosection

The geoelectrical litho section for each sounding curve is prepared based on the resistivity contrast of each layer after iteration (Fig. 3). The resistivity value of each layer is interpreted with the known values of different lithological units and geological information of the area (Fig. 4) (Telford et al., 1990). From the geoelectrical lithosection it is inferred that the area is composed of dolomite (Abbottabad formation) with intercalations of sandstone, clay and shale (Patala Formation). The subsurface geological sections are prepared at various depths (0 to 20 m, 20 to 100 m and 100 to 500 m) using the geoelectrical lithosection of each VES (Fig. 5). From geological sections it is inferred that at the western side, there is maximum amount of dolomite at the top and less shale, and on the eastern side the clayey sandy, shale lithology dominates. From this juxtaposition of different lithologies on the western and eastern side, there is a clear indication of fault or unconformity between Palaeocene Patala formation and Cambrian Abbottabad Formation, with zone of delineation along the river Poonch.

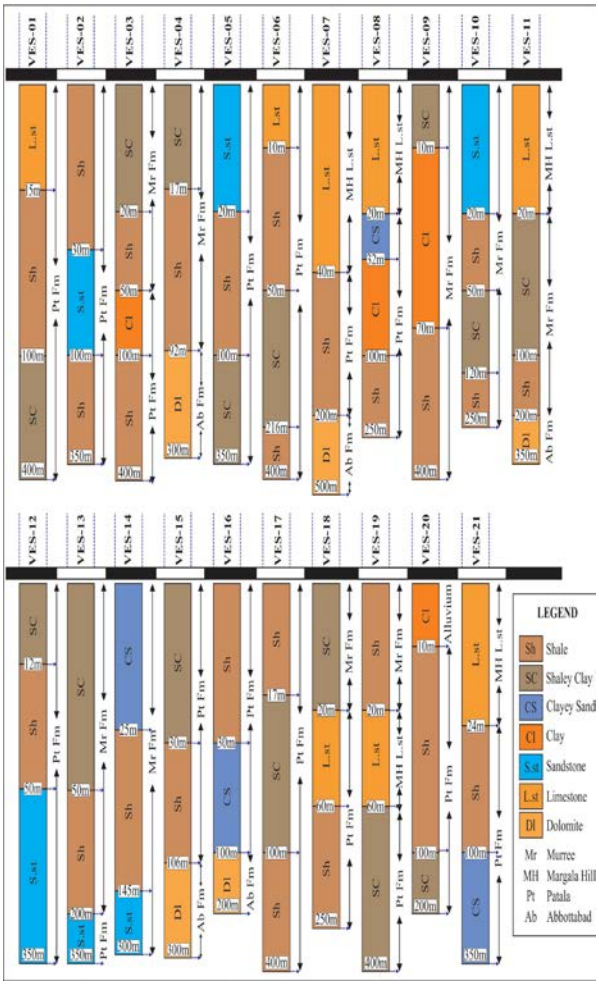

Fig. 3 Geoelectrical lithosections of VES-01 to VES-21.

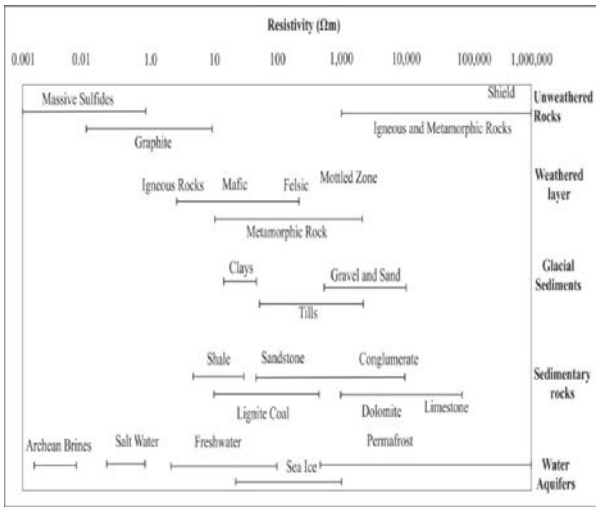

Fig. 4 Resistivity chart showing resistivity range of different geological materials (Telford et al., 1990).

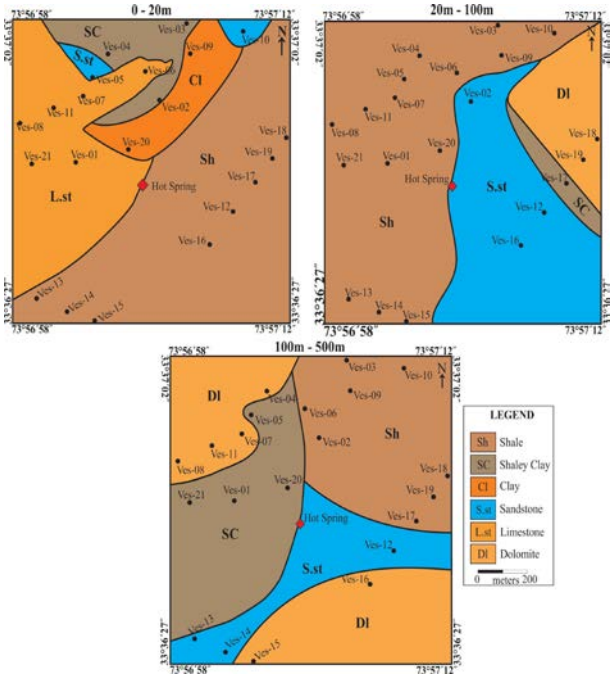

Fig. 5 Subsurface geological section of the study area.

Apparent Resistivity Sections

In order to have a clear indication of resistivity distribution at various promising depths of 10, 20, 60 80, 100 and 200 m depth, the iso-apparent resistivity maps are prepared by applying Kriging interpolation techniques using surfer software 10.1. The apparent resistivity distribution systematically changes with depth and four promising zones are delineated relating to resistivity contrast, such as high (≥300 Ωm), moderately high (100-200 Ωm), moderately low (50-100 Ωm), and very low resistivity (≤ 50 Ωm) (Fig. 6). The apparent resistivity shows a clear indication of fault zone where hot thermal spring is concentrated, demarcated at 10 m and 20 m depths with resistivity range of 20≤ρ≥150 Ωm (Fig. 6 a & b). At 60 m depth, which is the focal point of thermal spring (P-3), it is also demarcated by apparent resistivity low value in range of 20≤ρ≥70 Ωm (Fig. 6 c), with extension in N-S direction and is in conformation with the Pseudo section. It is evident from the apparent resistivity section that with increase in depth, the dolomite content decreases from the western side and shale content increase with depth (Fig. 6 d, e f), the same trend is shown by geoelectrical lithosection and geological cross section. There is also a clear indication that thermal hot plumes having low resistivity values (20 Ωm to 70 Ωm) are extending at a high rate in N-S direction, with inclination towards NE-SW side.

Pseudo Section

In order to have a clear picture of resistivity distribution and variation with depths, the pseudo sections are graphed along ten profiles. Pseudo sections have been generated for all collinear VES displayed along different profiles to portray the variation of resistivity along each VES with depth (Fig. 7).

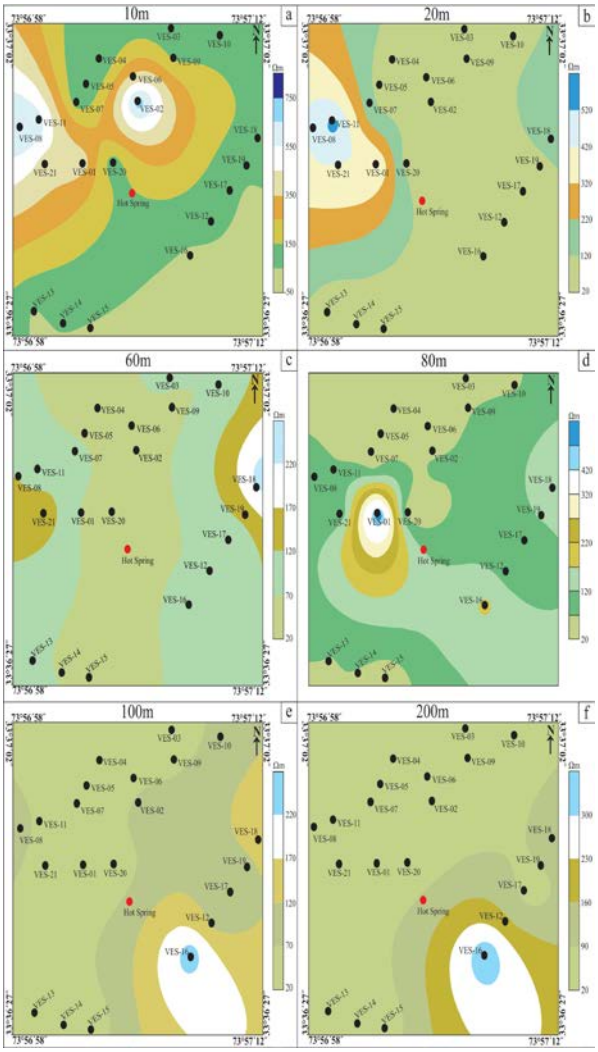

Fig. 6 Apparent resistivity distribution at 10, 20, 60, 80, 100 & 200 meters depth.

Four resistivity zones have been marked in pseudo-sections based on resistivity contrast i.e., Hot spring (HS) zone (ρ≤25 Ωm), Shale (Sh) (10≤ρ≥50 Ωm), Shaley Clay (Sh+Cl) (50≤ρ≥100 Ωm), Sandstone (S.st) (100≤ρ≥150 Ωm) and Dolomite (Dt) (ρ≥150 Ωm). The pseudo section revealed the presence of hot thermal spring at the depth of 60 m at VES-20 along P-3. The thermal spring and hot plumes are visible in each profile from P-1 to P-8. The general trend of plume migration is in NE-SW direction as visible in all sections. From the pseudo section, it is revealed that there is clear distinction of lithological unit P-1 to P-8 (dolomitic sequence) from P-9 to P-10 (shaley sequence). The pseudo section is in conformity with subsurface geoelectrical lithosection showing dominant lithology of dolomite on the western side and clayey sequence in the eastern side. The true resistivity values are also estimated from the inversion of apparent resistivity data for each VES and the results are shown in Table (1).

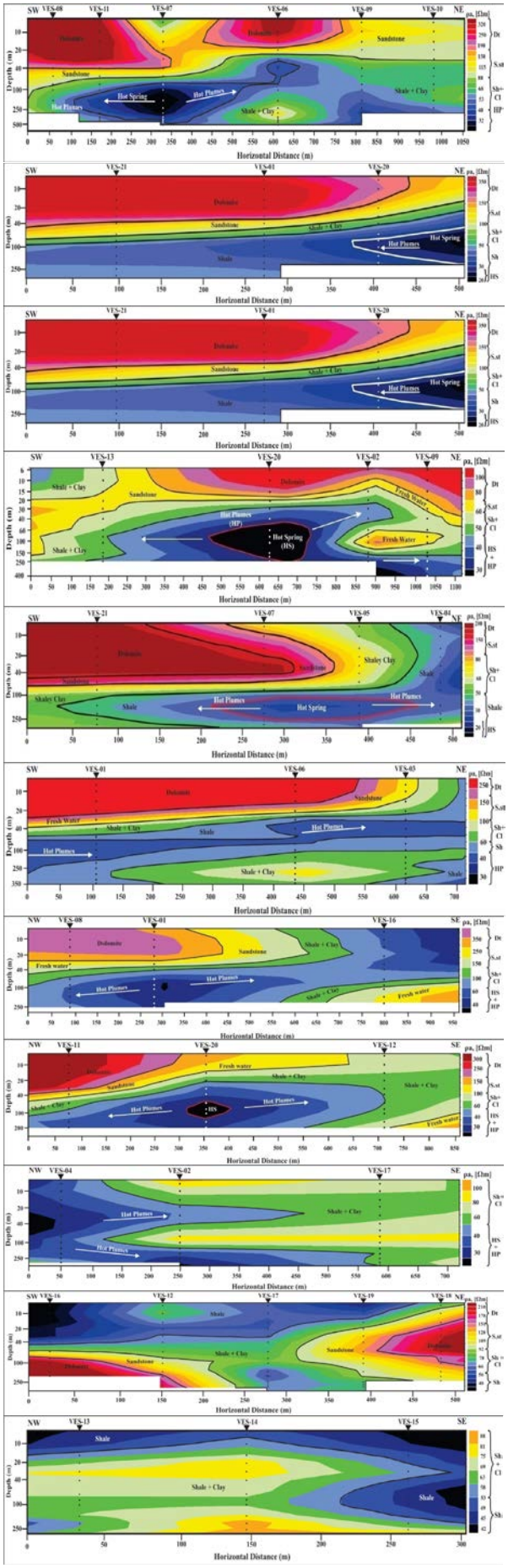

Fig. 7 Pseudo-section showing different geological units and migration of hot thermal plumes.

Statistical Distribution Curves

The mean Statistical Distribution Curves (SDC) of apparent resistivity are generated by simulation of statistical parameters in IPI2win software. The SDC along each profile is determined to decipher the trend of resistivity and lithological variation at depth (Fig. 8). The SDC is showing two trends, i.e. steep downward trend and gentle upward trend. From profile1 to -7, there is a steep dropdown trend, in which the lithologies commute in succession from dolomite (60≤ρ≥800 Ωm), sandstone (60≤ρ≥300 Ωm), shaley clay (60≤ρ≥250 Ωm) to shale (20≤ρ≥150 Ωm). The profile8 to -10 represent an upward gentle trend of resistivity, where lithology fluctuates between shale and clay. It is evident from SDC curves that there is an evident fault zone showing an abrupt variation of lithologies in adjacent vicinities, differentiating rocks on the eastern and western side of the study area. Also, the western side is having more permeable beds as lithological units of sandstone and dolomite, which favour the transport of hot plumes.

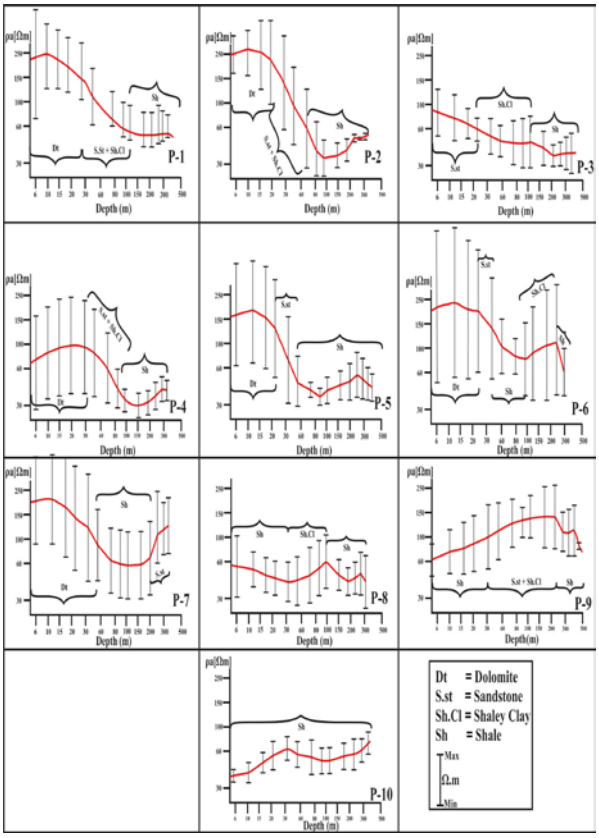

Fig. 8 Statistical Distribution Curve (SDC) showing trend of resistivity at depth along profile 1 to 10.

Characteristic of Geoelectrical Parameters\

The relationship between hydraulic conductivity and electrical conductivity was previously studied by various researchers and is more meaningful when dealing with water quality (Huntley, 1986; Niwas and Singhal, 1981).The two vital parameters that are describing the conductivity of a geological medium are

longitudinal unit conductance (S) and transverse unit resistance (TR) and macro anisotropy, which is defined by Dar Zarrouk Parameters (DZP) (Maillet, 1947). Transverse unit resistance and longitudinal conductance (S) differentiate the geological materials having high recharge capacity and it is considered the best site for water exploration (Iduma and Uko, 2016). Transverse unit resistance and longitudinal unit conductance maps are produced for the study area to have a clear picture for the recharge capability of geological fabric, which favors the flow of hot plumes.

The average total transverse unit resistance values range from 20-300 Ωm^2 (Fig. 9a). The general trend of TR is increasing in the NE and SW side of the study area, which will favour the flows of plumes. The minimum value of TR is recorded along VES-20, 13 and 5 within a limit of 20-40 Ωm^2. Along VES-20 the low TR is due to alteration of the rocks by hot plumes making it more permeable and conductive. The NE side of the study area is characterized by high resistance within a range of 140-300 Ωm^2. From the analysis of TR map, it is inferred that the NE and SW side around has a permeable layer encouraging flow of thermal water on either side.

The total longitudinal conductance (S) is the geo-electrical parameter used to demarcate areas of

Table 1 . Summary of VES analysis showing true resistivity of different layers.

VES	ρ (Ωm)	h (m)	D (m)	Layer
1	1375	9	15	Dolomite
	20	85	100	shale
	70	100		shaley clay
2	27	24	30	Shale
	292	70	100	Sandstone
	13	250		Shale
3	56	14	20	Shaley Clay
	25	30	50	Shale
	142	50	100	Clay
	17	293		Shale
4	57	11	17	shaley clay
	16	75	92	Shale
	7509	158		Dolomite
5	202	14	20	Sandstone
	10	80	100	Shale
	48	294		Shaley Clay
6	430	4	10	Dolomite
	21	40	50	Shale
	155	166	216	Shaley Clay
	12	184		Shale
7	359	34	40	Dolomite
	11	160	200	Shale
	1563	113		Dolomite
8	650	14	20	Dolomite
	225	12	32	clayey sand
	150	68	100	Clay
	30			Shale
9	131	4	10	Shaley Clay
	59	60	70	Clay
	36	69		Shale
10	205	14	20	Sandstone
	36	30	50	Shale
	150	70	120	shaley clay
	18			Shale

VES	ρ (Ωm)	T (m)	D (m)	Layer
11	770	14	20	Dolomite
	59	80	100	Shaley Clay
	12	100	200	Shale
	4518	113		Dolomite
12	78	6	12	Shaley Clay
	41	38	50	Shale
	218	30		Sandstone
13	116	46	50	Shaley Clay
	43	150	200	Shale
	225	214		Sandstone
14	150	19	25	Clayey Sand
	63	120	145	Clay
	278	145		Sandstone
15	59	24	30	Shaley Clay
	26	76	106	Shale
	857	106		Dolomite
16	39	24	30	Shale
	230	70	100	Clayey Sand
	2621	30		Dolomite
17	41	11	17	Shale
	111	83	100	Shaley Clay
	37		284	Shale
18	90	16	20	Shaley Clay
	402	40	60	Dolomite
	50	60		Shale
19	44	16	20	Shale
	222	40	60	Dolomite
	67	50		Shaley Clay
20	112	4	10	Clay
	35	40	50	Shale
	11	50	100	Shale
	67	100		Shaley Clay
21	403	18	24	Dolomite
	15	76	100	Shale
	61	48		Shaley Clay

groundwater potential based on unit resistivity over a known thickness. Areas characterized by high S values normally indicate a relatively thick conductive succession of good porosity. The S of the study area varies between 0.95-15 mohos (Fig. 9b) with high values of S (6-15mohos) observed in the north western side, showing more permeable beds, making it conductive. The moderate value of S (2 – 5 mohos) is observed in the SW side while low value (0.95-2 mohos) is observed in the NE-SE side. This indicates that NW and SW side is more permeable with maximum sandstone and dolomite, while NE-SE side shows porous beds of shales and clays. The macro-anisotropy map is prepared to decipher the major change in lithological fabric along the hot spring with value range (1-2.7) which indicates the fault having orientation in NE-SW direction, in conformation with geo-electrical and pseudo section (Fig. 9c).

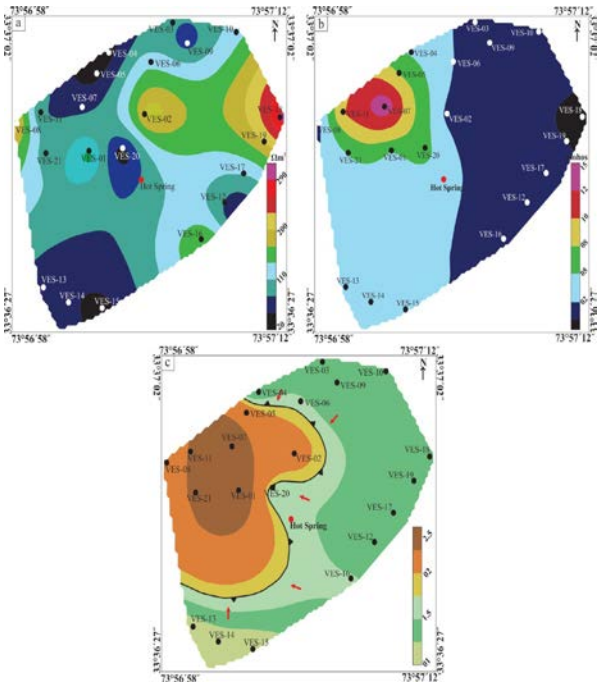

Fig 9 Geo-electrical Parameters showing hydraulic conductivity of the study area, (a) Transverse Resistivity, (b) Longitudinal Conductance, (c) Macro anisotropy.

Magnetic Map

Two types of magnetic maps are prepared to portray the magnetic properties of the rocks in the study area i.e. Total Magnetic Intensity Map (TMI) and Total Anomaly Map (TAM) (Fig. 10). The TMI map revealed that based on the magnetic intensity, two types of magnetic signatures (high and low) can be identified in the study area. The high magnetic values range between 50300 to 50450 nT, while a low magnetic zone has values between 50000 to 50300 nT. The total magnetic intensity field data are corrected by applying all necessary correction (Diurnal and Normal) to produce total anomaly map (TAM). The high magnetic anomalies value ranges between 10-120 nT and attributed to shaley clayey and sandy sequence, while low value in the range of -300 to 10 nT is attributed to the presence of dolomite. The TMI and TAM maps show the presence of thermal spring at the contact of two contrasting magnetic signatures inferring to fault zone and verifying the results of resistivity survey.

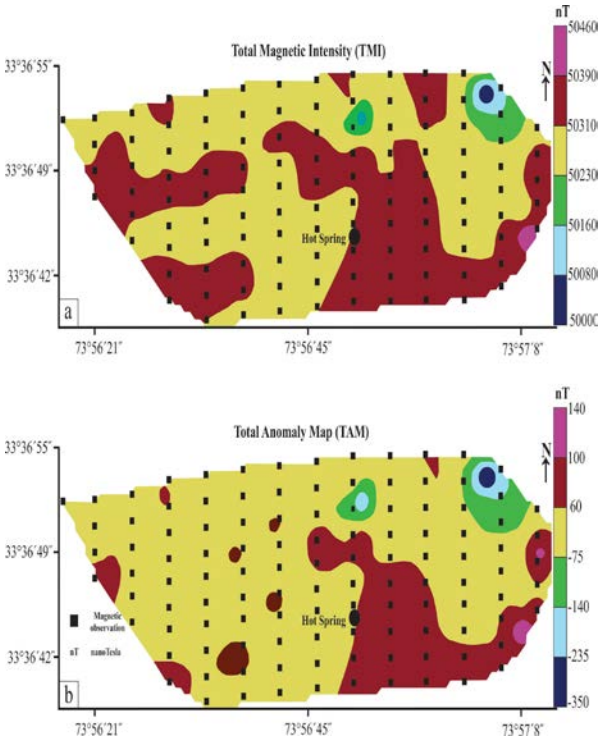

Fig. 10 Total Magnetic Intensity (TMI) and Total Anomaly Map (TAM) of the study area.

Conclusion

In the recent study 21 VES are interpreted to decipher the depth of thermal zone and extension of thermal plumes. The data shows that the thermal spring oozes at the contact of Abbottabad Formation (dolomite) and Patala Formation (shale + limestone ± sand). The western side of the study area is having more dolomite and sand as compared to eastern side favouring the plume migration. The thermal spring is having low resistivity within a range of ≥20 Ωm as shown by pseudo-section, with promising depth of 60 m (P-3). The extension of thermal plumes is more prominent in the NE and SW side mapped by pseudo section (P-1, P-2, P-3, P-4 and P-5). The apparent resistivity distribution shows that the promising narrow zone of thermal spring exists at 60 meters depth having an orientation of NNE to SSW. From statistical distribution curves it is inferred that the shaley content increases with depth due to alteration of the surrounding rock by thermal plumes. The fresh ground water is mostly concentrated at a depth of 20 to 40 m, mostly above the thermal zone and probable mixing of thermal and fresh water is making it undrinkable. The geo-electrical parameters also show moving of thermal plumes in the NE-SW direction, showing that directions are more prone to contamination, due to porous lithology. The magnetic signature is verifying

the geo-electrical results, showing fault bound thermal spring in which heat is driven by underground normal geothermal gradient. To delineate the deep seated tectonic and structure of thermal hot spring, semi-detail gravity and magnetic surveys of the surrounding area are recommended. It is also of vital interest to have complete geochemical and isotopic analysis of thermal water to compute for subsurface reservoir temperature. It is also concluded to have deep drilling up to 1000 m on the left bank of river Poonch in the NE direction to puncture the entire thermal zone to have the geological and geochemical control of thermal spring.

Acknowledgement

This work was funded by a Ministry of Energy (Petroleum Division) and Geoscience Advance Research Laboratories (GARL) Geological Survey of Pakistan (GSP) Islamabad (Project no GSP-GARL-03-2016-2017).

References

Ahmad, M., Akram, W., Ahmad, N., Tasneem, M. A., Rafiq, M., Latif, Z. (2002). Assessment of reservoir temperatures of thermal springs of the northern areas of Pakistan by chemical and isotope geothermometry. *Geothermics*, **31**(5), 613-631.

Akaninyene, O., Igboekwe, M. (2012). Preliminary lithologic deductions for michael Okpara university of agriculture, Umudike, Abia state, Nigeria, using Vertical Electrical Sounding Method. *Arch. Phy. Res.*, **3**(4), 292-302.

Anees, M., Shah, M. M., Qureshi, A. A. (2015). Isotope studies and chemical investigations of Tattapani hot springs in Kotli (Kashmir, NE Pakistan): Implications on reservoir origin and temperature. *Procedia Earth and Planetary Science*, **13**, 291-295.

Araffa, S. A. S., Santos, F. A. M., Arafa-Hamed, T. (2012). Delineating active faults by using integrated geophysical data at northeastern part of Cairo, Egypt. *NRIAG Journal of Astronomy and Geophysics*, **1** (1), 33-44.

Arshad, M., Cheema, J., Ahmed, S. (2007). Determination of lithology and groundwater quality using electrical resistivity survey. *International Journal of Agriculture and Biology*, **9** (1), 143-146.

Atakpo, E. A., Ayolabi, E. A. (2009). Evaluation of aquifer vulnerability and the protective capacity in some oil producing communities of western Niger Delta. *The Environmentalist*, **29** (3), 310-317.

Bakht, M. S. (2000). An overview of Geothermal Resources of Pakistan. *Proceedings World Geothermal Congress*, 77-83.

Bobachev, C. IPI2Win. (2002). A windows software for an automatic interpretation of resistivity sounding data. Thesis, Moscow State University, Moscow, Russia.

Bradbury, K. R., Taylor, R.W. (1984). Determination of the hydrogeologic properties of lake beds using offshore geophysical surveys. *Groundwater*, **22** (6), 690-695.

El All, E.A., Khalil, A., Rabeh, T., Osman, S. (2015). Geophysical contribution to evaluate the subsurface structural setting using magnetic and geothermal data in El-Bahariya Oasis, Western Desert, Egypt. *NRIAG Journal of Astronomy and Geophysics*, **4** (2), 236-248.

Gassert, F., Reig, P., Luo, T., Maddocks, A. (2013). Aqueduct country and river basin rankings: a weighted aggregation of spatially distinct hydrological indicators. World Resources Institute, *http://wri. org/publication/aqueduct-country-river-basin-rankings*.

He, L., Hu, X., Zha, Y., Xu, L., Wang, Y. (2014). Distribution and origin of high magnetic anomalies at Luobusa Ophiolite in Southern Tibet. *Chinese Science Bulletin*, **59** (23), 2898-2908.

Hewaidy, A. G. A., El-Motaal, E. A., Sultan, S. A., Ramdan, T. M., khafif, A. A. E., Soliman, S. A., Dilek, Y. (2015). Groundwater exploration using resistivity and magnetic data at the northwestern part of the Gulf of Suez, Egypt. *Egyptian Journal of Petroleum*, **24**, 255-263.

Huntley, D. (1986). Relations between permeability and electrical resistivity in granular aquifers. *Groundwater*, **24** (4), 466-474.

Iduma, R. E. O., Uko, E. D. (2016). Dar Zarrouk parameter as a tool for evaluation of well locations in Afikpo and Ohaozara, southeastern Nigeria. *Journal of Water Resource and Protection*, **8**(4), p.505.

Joshua, E. O., Odeyemi, O. O., Fawehinmi, O. O. (2011). Geoelectric investigation of the groundwater potential of Moniya Area, Ibadan. *Journal of Geology and Mining Research*, **3**(3), 54-62.

Koukadaki, M. A., Karatzas, G. P., Papadopoulou, M. P., Vafidis, A. (2007). Identification of the saline zone in a coastal aquifer using electrical tomography data and simulation. *Water Resources Management*, **21** (11), 1881-1898.

Kundu, N., Panigrahi, M., Sharma, S., Tripathy, S. (2002). Delineation of fluoride contaminated groundwater around a hot spring in Nayagarh, Orissa, India using geochemical and resistivity studies. *Environmental Geology*, **43** (1), 228-235.

Maillet, R. (1947). The fundamental equations of electrical prospecting. *Geophysics*, **12** (4), 529-556.

Maury, S., Balaji, S. (2014). Geoelectrical method in the investigation of groundwater resource and related issues in Ophiolite and Flysch formations of Port Blair, Andaman Island, India. *Environmental Earth Sciences*, **71** (1), 183-199.

Mughal, M. N., Khan, R., Hussain, A. (2004). Geological map of the Kotli Area, part of Kotli and Sudhonti districts AJK. Geological Survey of Pakistan Quetta.

Nadeem, F. (2015). Pakistan monsoon rainfall. *CDPC Technical Report*, **2**, 4 pages.

Niwas, S., Singhal, D. C. (1981). Estimation of aquifer transmissivity from Dar-Zarrouk parameters in porous media. *Journal of Hydrology*, **50**, 393-399.

Ojelabi, E., Badmus, B., Salau, A. (2002). Comparative analysis of Wenner and Schlumberger methods of geoelectric sounding in subsurface delineation and groundwater exploration-A case study. *Geological Society of India*, **60** (6), 623-628.

Oseji, J., Asokhia, M., Okolie, E. (2006). Determination of groundwater potential in obiaruku and environs using surface geoelectric sounding. *Environmentalist*, **26** (4), 301-308.

Shah, S. A. H., Irfan, S. M., Khan, M. A., Sharaz, M., Sadiq, M., Khokhar, F. K., Sultan, K. (2004). Report of Water Quality Monitoring in Azad Jammu & Kashmir; Public Health Engineering, 1-44.

Shah, S. H., Abbas, Q., Tariq, M., Mehmood, Z. (2007). Geological map of Tatta Pani coal field, district Kotli, Azad Kashmir. Publication Directorate GSP, Quetta, Geological Map Series No. 2.

Shah, S. M. I. (2009). Stratigraphy of Pakistan: 22nd ed.; Geological Survey of Pakistan Publication Directorate: Quetta Pakistan, **22**, 381 pages.

Sikandar, P., Bakhsh, A., Arshad, M., Rana, T. (2010). The use of vertical electrical sounding resistivity method for the location of low salinity groundwater for irrigation in Chaj and Rachna Doabs. *Environmental Earth Sciences*, **60** (5), 1113-1129.

Stollar, R.L., Roux, P. (1975). Earth resistivity surveys: A method for defining ground water contamination. *Ground Water*, **13** (2), 145-150.

Sultan, S. A., Santos, F. A. M. (2008). Evaluating subsurface structures and stratigraphic units using 2D electrical and magnetic data at the area north Greater Cairo, Egypt. *International Journal of Applied Earth Observation and Geoinformation*, **10** (1), 56-67.

Telford, W. M., Geldart, L. P., Sheriff, R. E. (1990). Applied geophysics: Cambridge University Press: Cambridge, 770 pages.

Thakur, V., Jayangondaperumal, R., Malik, M. (2010). Redefining Medlicott–Wadia's main boundary fault from Jhelum to Yamuna: An active fault strand of the main boundary thrust in northwest Himalaya. *Tectonophysics*, **489** (1), 29-42.

Todaka, N., Shuja, T.A., Jamiluddin, S., Khan, N.A., Pasha, M.A., Iqbal, M.A. (1988). preliminary Study of Geothermal Energy Resources of Pakistan. Geological Survey of Pakistan, Quetta.

Rao, V. G., Kalpana, P., Rao, R. S. (2014). Groundwater investigation using geophysical methods-A case study of Pydibhimavaram industrial area. *International Journal of Research in Engineering and Technology*, **3**, 13-17.

Wilson, S. R., Ingham, M., McConchie, J. A. (2006). The applicability of earth resistivity methods for saline interface definition. *Journal of Hydrology*, **316** (1), 301-312.